Carbohydrate Polymers 92 (2013) 591–597

Contents lists available at SciVerse ScienceDirect

Carbohydrate Polymers

journal homepage: www.elsevier.com/locate/carbpol

Cardiac repair using chitosan-hyaluronan/silk fibroin patches in a rat heart model with myocardial infarction

Nai-Hsin Chi[a,1], Ming-Chia Yang[a,1], Tze-Wen Chung[b,*], Nai-Kuan Chou[a], Shoei-Shen Wang[a,**]

[a] Department of Surgery, National Taiwan University Hospital, College of Medicine, National Taiwan University, Taipei, 100 Taiwan, ROC
[b] Department of Chemical Engineering, National Yunlin University of Science and Technology, Dou-Liu, Yun-Lin, 640 Taiwan, ROC

ARTICLE INFO

Article history:
Received 21 June 2012
Received in revised form 6 September 2012
Accepted 7 September 2012
Available online 16 September 2012

Keywords:
Chitosan-HYA/SF cardiac patch
Cardiac repair
Myocardial infarction
Angiogenesis
Paracrine factors

ABSTRACT

The cardiac repair of myocardial infarction (MI) hearts of rats using chitosan-hyaluronan/silk fibroin (chitosan-HYA/SF) cardiac patches was examined after eight weeks of implantation. Rats with implantations of chitosan-HYA/SF patches (CHS group) significantly ($P < 0.05$) reduced the dilation of the inner diameter of left ventricle (LV) (4.27 ± 0.29 mm), increased wall thickness of LV (1.5 ± 0.13 mm) and improved the fractional shortening of LV of hearts (LVFS) ($42.8 \pm 2.4\%$) compared with those values of LVs of rats without implants (MI group) (e.g., 5.92 ± 0.39 mm, 1.2 ± 0.06 mm and $31.5 \pm 1.4\%$, respectively). Moreover, blood vessel-like structures in MI regions of LVs in the CHS group were widely distributed while none was found in the MI group. The CHS group significantly improved the secretion of paracrine factors, such as VEGF in the MI regions of LVs ($P < 0.05$, $n = 4$), relative to that in the MI group. In conclusion, chitosan-HYA/SF cardiac patches are promising biomaterials for the cardiac repair of MI rat hearts.

1. Introduction

Myocardial infarction (MI), a leading cause of heart failure, results in injury of the myocardium, gradual loss of cardiac tissue and impairment of left ventricular (LV) functions by impairment of ventricular remodeling, such as by wall thinning and scar formation (Van Lenthe, Gevers, Joung, Bosma, & Mackenbach, 2002). One of the therapeutic strategies involves attenuation of progressive remodeling, leading to tissue destruction following MI (Yang et al., 2007). Various biomaterials that exhibit both mechanical and biochemical functions that improve the LV remodeling of MI hearts are worthy of development.

Several materials have been investigated for use in post-MI remodeling. For instance, there are glutaraldehyde-crosslinked membranes such as bovine pericardium (Kochupura et al., 2005; Robinson et al., 2005), woven nylon for use in cardiac-restraining devices (Yamazaki et al., 1989) and expanded poly-tetrafluoroethylene (e-PTFE) (Minatoya et al., 2001). Although the aforementioned membranes or devices improve LV remodeling, they are not typically biodegradable and most induce immunoresponses of various strengths (Jin et al., 2009; Piao et al., 2007). Recently, alginate or chitosan hydrogels have been employed to improve heart remodeling and the functionality of chronic MI in rats or pigs (Leor et al., 2009; Lin et al., 2010; Lu et al., 2010). Although the benefits of remodeling MI hearts by treating them with hydrogels have been established, their efficacies are usually influenced by gel volume, location of injection, and the mechanical strength of the injected hydrogel (Nelson, Ma, Fujimoto, Hashizume, & Wagner, 2011). Although some investigators have shown the efficacies of synthetic cardiac patches or scaffolds (such as poly (lactide-co-ε-caprolactone) scaffolds) in the remodeling of MI hearts (Jin et al., 2009; Piao et al., 2007), studies of the efficacy of cardiac patches that are fabricated from chitosan-HYA/SF on the cardiac repair of MI rat hearts are lacking.

Chitosan, an amino polysaccharide, is suitable for the preparation of complex matrices for tissue engineering, such as in the neo-formation of bone and cardiomyogenesis (Muzzarelli et al., 1994; Muzzarelli, 2009; Rios, Skoracki, Miller, Satterfield, & Mathur, 2009; Yang et al., 2009). Moreover, it has a chemo-attractive property for growth factors, and high capacity to form complexes with inorganic and biochemical substances in the repair of wounded skin and the regeneration of nerves and bone (Minatoya et al., 2001; Muzzarelli, 2011). Hyaluronan is distributed throughout the ECM of connective tissues of humans and other mammals. Furthermore, HYA promotes wound healing (Dechert, Ducale, Ward, & Yager, 2006) and can be incorporated with other biomaterials including chitosan and chondroitin sulphate to produce hybrid matrices for promoting angiogenesis, and for the regeneration of cartilage

* Corresponding author. Tel.: +886 5 5342601 4610; fax: +886 5 5312071.
** Co-corresponding author.
E-mail address: twchung@yuntech.edu.tw (T.-W. Chung).
[1] Co-first author.

0144-8617/$ – see front matter © 2012 Elsevier Ltd. All rights reserved.
http://dx.doi.org/10.1016/j.carbpol.2012.09.012

(Muzzarelli, 2012; Perng, Wang, Tsi, & Ma, 2011). The interactions between CD44 of HYA and the receptors of the bone marrow stem cells (BMSC) of rats are reportedly important in the cardiomyogenesis of the cell (Yang et al., 2009, 2010). SF, a fibrous protein that comprises glycine and alanine as the main amino acid residues, has been extensively examined for engineering tissues, such as tendon regeneration, because of its low inflammatory response and favorable biological response (Kardestuncer, McCarthy, Karageorgiou, Kaplan, & Gronowicz, 2006; Meinel et al., 2005). Chitosan-HYA/SF cardiac patches incorporated chitosan-HYA into SF, and supported the proliferation of bone marrow stem cells (BMSC) and their differentiation into cardiomyocytes in an in vitro study (Yang et al., 2009, 2010). For instance, in vitro cardiomyogenic differentiations of BMSC on chitosan-HYA/SF patches were significantly higher in expressing cardiomyocyte-specific proteins such as troponin T and cardiac genes such as Nkx2.5 than those on SF patches (Yang et al., 2009, 2010). Hence, the effectiveness of chitosan-HYA/SF patches on cardiac repair in vivo is thereby examined herein using an MI rat heart model.

This study is to examine the influences of implanting chitosan-HYA/SF patches on cardiac repair of MI rat hearts. Chitosan-HYA/SF patches were fabricated by this laboratory as described elsewhere (Yang et al., 2009, 2010). The model of an MI rat heart was induced using a cryo-injury technique (Jin et al., 2009; Van den Bos, Mees, de Waard, de Crom, & Duncker, 2005). To evaluate the cardiac repair of MI rat hearts with implanting chitosan-HYA/SF patches, the patches were first implanted to the MI zones of LVs, and the cardiac functions including LV fractional shortening (LVFS) and the end-diastolic diameters of hearts were assessed by echocardiography and catheterization, respectively, in 2 months after the implantation. In addition, the vWF immunochemical staining was carried out to examine the vessel-like formations in the MI zone of an LV. The secretions of various paracrine factors in the MI zone of an LV such as vascular endothelial growth factor (VEGF), basic fibroblast growth factor (bFGF) and hepatic growth factor (HGF) were also determined by a real-time PCR.

2. Materials and methods

2.1. Fabricating chitosan-HYA/SF patches

The procedures for producing chitosan-HYA/SF patches were followed as our early reports (Yang et al., 2009, 2010). Briefly, silk cocoons were purchased from a silk center in Taiwan (ShihTan, Miao-Li, Taiwan), boiled in Na_2CO_3 and SF was extracted. SF was then dissolved in 9.3 M LiBr solution and then dialyzed. The final concentration of the SF aqueous solution was 8% (w/v). Chitosan (96% de-acetylated; MW, 200 kDa) (Sigma–Aldrich, USA) and hyaluronan (HYA) (MW, 15 kDa) (Lifecore, USA) were added and dissolved in the previously SF solution (1.5 wt%) to yield the ratios of chitosan-HYA/SF (w/w/w) as 1:1:10 (Yang et al., 2009, 2010). To prepare the patches, the SF-based hybrid microparticles were initially fabricated using a spray-drying machine (EYERS SD-1000) (Tokyo Rikakikai Co., Tokyo, Japan). These microparticles were then pressed using a pressing machine at a pressure of 10 GPa at room temperature to fabricate chitosan-HYA/SF patches. The chitosan-HYA/SF patches were then crosslinked in 1% genipin solution (Challenge Bio-products Co., Ltd., Taipei, Taiwan) for 12 h at 45 °C; the cross-linking reactions were terminated by adding 3% glycine. The dark-blue patches had a diameter of 13 mm, thickness of 200 mm, and mass of 20–25 mg, and swelling ratio of 15–20%. The patches were put in a bottle of distillated water and the bottle was sterilized by an autoclave at 121 °C for 40 min which were ready for animal studies.

2.2. Experimental animals

Thirty female Wistar rats weighing around 250 g were housed and maintained in a controlled environment. All procedures involving animals were approved by the Animals Committee of the National Taiwan University College of Medicine. Rats were divided into three experimental groups (Fig. 1): the sham group ($n = 6$); which thoracotomy was performed without a cryo-injured treatment; the MI group ($n = 13$); which the MI model was provoked (Jin et al., 2009; Van den Bos et al., 2005); the CHS group ($n = 11$); the chitosan-HYA/SF patches were implanted onto MI rat hearts.

To induce MI in a rat heart, the following cryo-injury procedures were performed (Jin et al., 2009; Van den Bos et al., 2005); Rats were anesthetized and subsequently intubated and ventilated mechanically with room air. The heart was exposed through a left thoracotomy (in third or four inter-costal spaces) and an LV acute MI was created using three sequential exposures to a liquid-nitrogen-cooled cryo-probe, a stainless-steel cylinder with 6 mm in diameter. Initiation of MI of heart was confirmed by wall blanching followed by hyperemia (Callegari et al., 2007; Jin et al., 2009; Treguer et al., 2010; Van den Bos et al., 2005). Moreover, the cryo-injury zone of an MI heart was identified by their pale color relative to that of the surrounding myocardium.

2.2.1. Implanting chitosan-HYA/SF patches onto MI hearts

The chitosan-HYA/SF patches were then placed on the epicardial anterolateral region corresponding to the injured area (about 30 mm^2). After MI hearts were successfully induced and stabilized, the patches cut in size of 8 mm × 8 mm were covered on the epicardial anterolateral region where was correspondent to the cryo-injured area. The cardiac patches were fixed to the MI zones by fibrin glue (OMRIX Biopharmaceuticals Ltd., USA) in four positions of their edges. The results of cardiac repairs of MI hearts for all study groups were examined after the rats were sacrificed in the end of study.

2.3. Histology, histochemistry and morphometry of MI hearts

Frozen sections of 5 μm thick were cut from MI zone of the rat hearts in the four experimental groups and stained with hematoxylin and eosin (HE) and massom trichrome stain (MT) for immunohistological analysis. Their morphology was observed using a phase contrast microscope that was equipped with fluorescent light and photographs were taken using a CCD camera (Zeiss Axioskop2, Germany). The LV inner diameter in transverse section across the LV of HE staining specimen was measured at the level of mid portion of papillary muscle and counted by two blinded observers in five slides; the mean number of HE staining per specimen was used for analysis. For histochemistry analyses, five equatorial sections of the MI zones of LVs were reacted with anti-Von Willebrand factor (vWF; for capillaries) (Millipore, CA, USA), anti-alpha-myosine heavy chain (anti-α-MHC; mouse IgG in 1:200; for stains of contract proteins) (Millipore, CA, USA) and CD68 (Millipore, CA, USA) for each cardiac sample of an animal.

2.4. LV functional evaluations for MI hearts

Trans-thoracic echo-cardiographies of rats were performed before MI induced to obtain a baseline echocardiogram, and at eight weeks after MI induction. Rats were anesthetized with 150 mg/kg barbiturate after echocardiographic examination. A commercial echocardiographic machine with a 15 MHz linear transducer was used to evaluate LV dimensions and systolic function. Under the left lateral decubitus position, M-mode tracing of the LV was obtained close to the papillary muscle level using the short-axis imaging

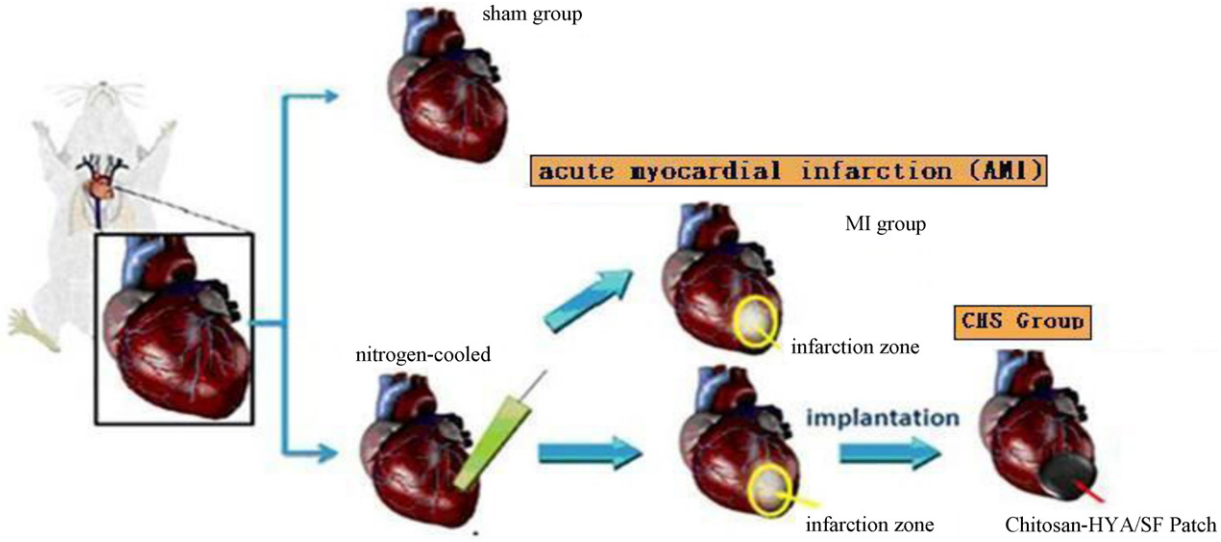

Fig. 1. Schematic illustrations of the study groups including the sham, MI and CHS (MI hearts with implantation of CS-HA/SF patches). An MI rat heart was induced by a cryo-injury technique with a nitrogen-cooled probe (the green bar). (For interpretation of the references to color in this figure legend, the reader is referred to the web version of this article.)

plane. All the dimensions and wall thickness data of LV were measured according to the American Society of Echocardiography leading-edge technique, and the value of each rat was the mean of three measurements. In addition, the fractional shortening (FS) of the LV is expressed as FS (%). The LV fractional shortening (LVFS) was expressed as: LVFS (%) = [LV internal dimension on end diastole ((LVID) d) − internal dimension on end systole ((LVID) s)/(LVID) d] × 100. All measurements are averages of three consecutive cardiac cycles and were made by an experienced technician blind to the treatment groups.

2.5. Total RNA and real-time PCR analysis for MI zones of hearts

The mRNA populations were determined by real-time polymerase chain reaction (PCR) analysis using a TaqMan primer-probe, TaqMan Universal PCR master mix, and automated fluorometer (ABI Prism 7900) as our early reports (Yang et al., 2009, 2010). In brief, rat hearts of four rats of each group were randomly selected for the real-time PCR analysis. 0.5 g of a cardiac tissue in the MI zone of a heart was first homogenized at 4 °C, centrifuged and the pellet in the bottom was obtained for the PCR analysis. Total RNA was extracted from cells using an RNeasy Mini Kit (Qiagen, Hilden, Germany) following the manufacturer instructions. Total concentration of extracted RNA was determined by UV spectroscopy at OD260 nm and an RNA sample for RT-PCR analysis was repeatedly performed for three times or more (Yang et al., 2009, 2010). The quantifications of the expressions of various paracrine factors such as VEGF and bFGF in MI zones of LVs were analyzed by the RT-PCR technique (Yang et al., 2009, 2010). Customized probe-based TaqMan gene expression was performed using an ABI 7900 Sequence Detection System (Applied Bio-systems, Foster City, CA, USA). The detailed procedures for determining gene expressions can be referred elsewhere (Yang et al., 2009, 2010). The genes expression levels of Myh6 (Rn00568304_m1, myosin, heavy chain 6, cardiac muscle, alpha), VEGF (Rn01511601_m1, VEGF A), bFGF (Rn00570809_m1, FGF 2) and HGF (Rn00566673_m1, HGF) in MI zones were measured. The changes in values of gene expressions of the studied samples relative to the control were calculated (Pinhasov et al., 2004).

2.6. Statistical analysis

Statistical analyses for the experimental data of this study were employed with SigmaStat statistical software (Jandel Science Corp., San Rafael, CA, USA) (Yang et al., 2009, 2010). Statistical significance in the ANOVA analysis corresponded to a confidence level of at minimum 95%. Data are presented as mean ± SD of various measurements.

3. Results and discussion

3.1. MI rat hearts induced by a cryo-injury technique

Five of 13 rats in the MI group and three of 11 rats in the CHS group died intra-operatively and/or during the immediate postoperative period owing to surgical complications; no late postoperative death occurred in those groups. Accordingly, eight rats received chitosan-HYA/SF patches, which were directly implanted onto the infarcted zones of MI hearts. In this study, blanching wall followed by hyperemia of hearts was observed as an index for confirming that the cryo-injury technique successfully induced the MI rat hearts (Callegari et al., 2007; Jin et al., 2009; Treguer et al., 2010; Van den Bos et al., 2005). Moreover, the cryo-injured area of each MI heart was identified by its paleness relative to the surrounding myocardium (Fig. 2(a)). A similar technique was also utilized to induce the MI of hearts by others when they examined the effectiveness of synthetic polymer cardiac patches on cardiac repairs (Jin et al., 2009). Although the myocardial necrosis and scar formation in the MI zones that were caused by a cryo-injury model may be less similarity to those in clinical outcomes than those caused by coronary ligation, the size of the infarcted zone and the severity of myocardial dysfunction that are caused by cryo-injury are more controllable than those caused by ligation (Li et al., 1996; Van den Bos et al., 2005).

3.2. Cardiac functions of LV of MI hearts

3.2.1. Inner diameters of LV in MI hearts with or without implanted patches

Chitosan-HYA/SF patches promoted the proliferation and cardiomyogenic differentiation of BMSC of rats more effectively than

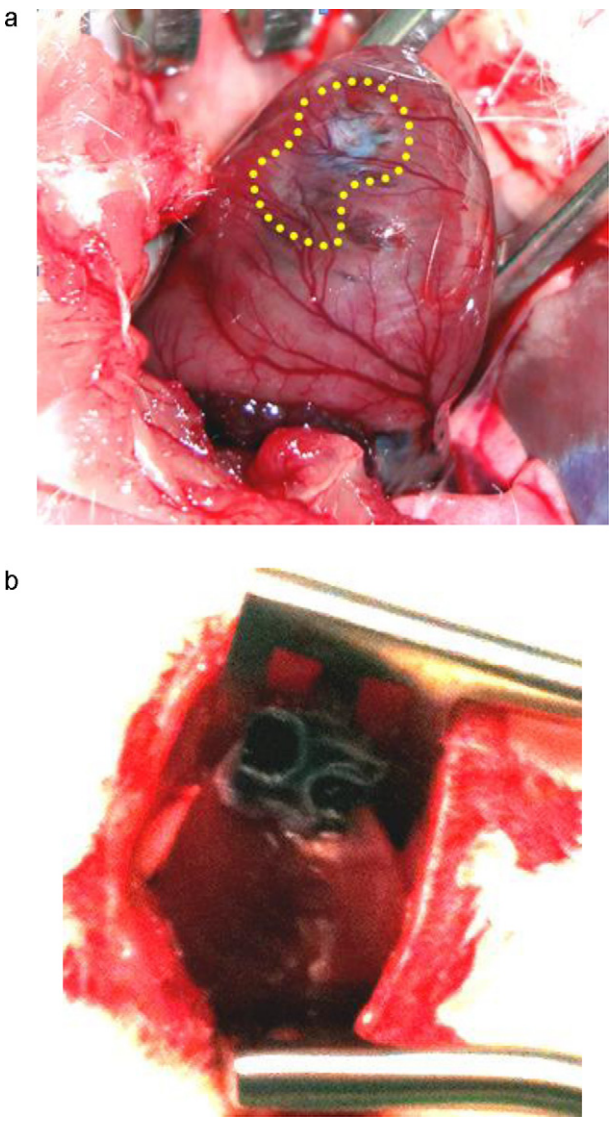

Fig. 2. The images of MI hearts: (a) the injured myocardium was shown after MI induced by a cryo-injury technique (within a yellow dashed line) and MI region in the apex area and (b) the morphology of a CS-HA/SF patch on the MI regions of the hearts after 2 months of study which was still adhered on the same place. (For interpretation of the references to color in this figure legend, the reader is referred to the web version of this article.)

did SF patches in vitro (Yang et al., 2009, 2010). The effectiveness of chitosan-HYA/SF patches in the cardiac repair of MI rat hearts is examined herein. After 2 months of study, chitosan-HYA/SF patches were still strongly attached to the MI regions of the hearts; they were morphologically intact without degradation and no aneurysm was observed around these regions, although they were partially covered by fatty connective tissues around the edges of the patches, perhaps because the implanted patches were directly covered onto the MI zones, and they were only fixed by fibrin glue at their edges (Figs. 2(b) and 3(c)). Furthermore, at the end of study, the patches generally exhibited a weak immuno-response, as determined by the immunochemical staining of an immuno-responsive CD-68 marker (data not shown), in the implantation regions.

Fig. 3(a)–(c) presents the HE staining of MI rat hearts in the three groups. The hearts that were obtained from rats of the sham group were intact. The inner diameter of the LV in a sample was indicated by an arrow (Fig. 3(a)). The hearts of the MI group exhibited extensive fibrous tissues; their LVs had enlarged inner diameters and the thickness of the walls in their MI regions was reduced (Fig. 3(b)).

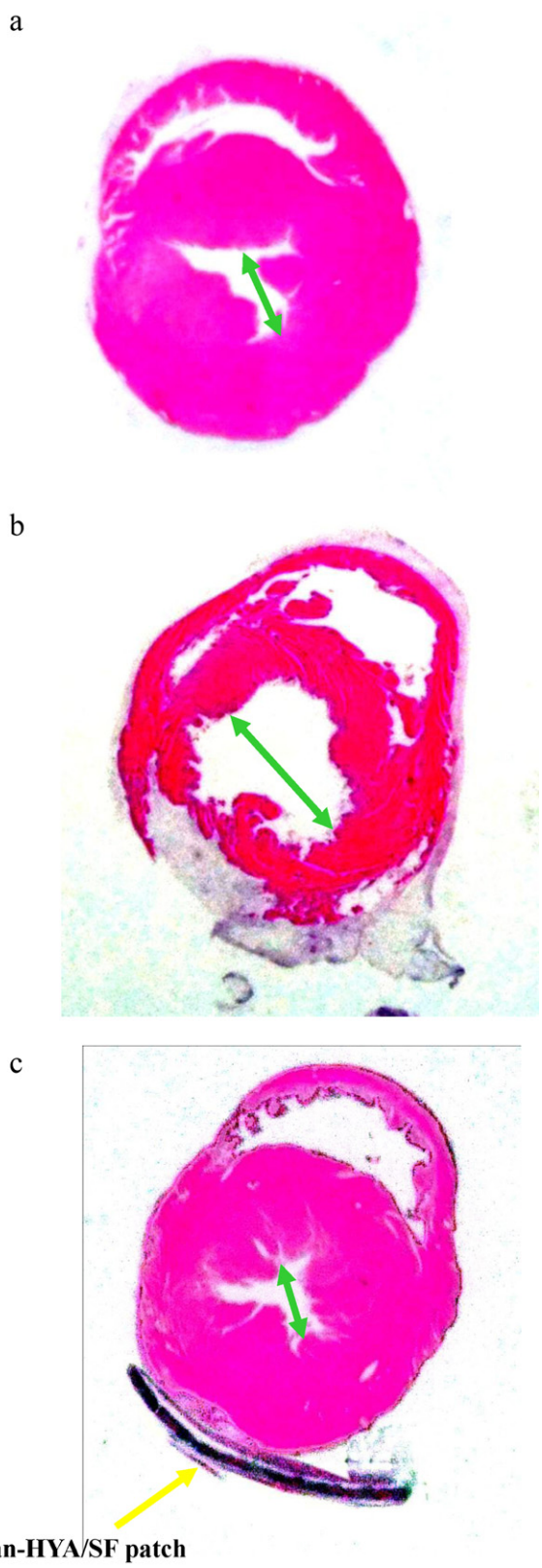

Fig. 3. HE stains of hearts of the (a) Sham, (b) MI and (c) CHS groups after eight weeks of study. The inner diameters of the LV of various study groups were shown by arrows. LV inner diameter of MI hearts in the MI group was significant larger compared with those of other groups.

Table 1
Hearts repair of LVs were evaluated with LV inner diameter, LVFS and LV wall thickness of MI hearts of three groups for eight weeks of study. LV inner diameters of the sham and CHS groups were significantly smaller than that of MI group although that of the sham group was significantly smaller than the CHS group (***$P < 0.001$, $n = 5$, respectively). The LVFS value of the CHS group was significantly higher than that of the MI group although that was lower than that of the sham group. Wall thickness of LVs of the CHS group was markedly thicker than that of the MI group although that was markedly thinner than the sham group (*$P < 0.05$; **$P < 0.01$; $n = 8$, respectively).

	Sham group	CHS group	MI group
LV inner diameter (mm) ($n = 5$)	$2.93 \pm 0.26^{***}$	$4.27 \pm 0.29^{***}$	$5.92 \pm 0.39^{***}$
LVFS (%) ($n = 8$)	$62.5 \pm 2.5^{**}$	$42.8 \pm 2.4^{**}$	$31.5 \pm 1.4^{**}$
Wall thickness (mm) ($n = 8$)	$3.40 \pm 0.15^{**}$	$1.50 \pm 0.13^{*}$	$1.20 \pm 0.06^{*}$

Of interest, the HE staining of MI hearts in the CHS group revealed that the inner diameters in the LVs were smaller than those in the MI group whereas the thicknesses of their walls exceeded those in the MI group (Fig. 3(b) and (c)). For instance, the inner diameters of the LVs in the CHS group (4.27 ± 0.29 mm, $n = 5$, respectively), measured using Vernier calipers, were significantly smaller than those in MI group (5.92 ± 0.39 mm, $n = 5$), revealing effective attenuation of LV remodeling of post-MI by the patches (Table 1). The mean measured inner diameters of the LVs in study groups were consistent with the observations of HE stains (Fig. 3 (a)–(c)). The inner diameters of the LVs in the CHS group were significantly smaller than those in the MI group, as in studies conducted by other groups, although those other studies involved other biomaterials such as PLCL scaffolds or cell sheets (Fujimoto et al., 2007; Jin et al., 2009; Miyahara et al., 2006; Piao et al., 2007). Treating MI rat hearts with mechanical supports, such as a woven nylon cardiac restraint or PLCL patches, can also reduce LV diameter and improve some cardiac functions (Jin et al., 2009; Minatoya et al., 2001; Piao et al., 2007; Yamazaki et al., 1989). In this work, the reduction of the diameters of LVs in MI hearts by implanting chitosan-HYA/SF patches demonstrated the benefits of a patch to provide mechanical support (Fig. 3). Moreover, the biochemical effects of chitosan-HYA/SF patches in the treatment of MI hearts, including the promotion of angiogenesis and the stimulation of the secretions of paracrine factors such as VEGF in MI hearts, were also elucidated.

3.2.2. Histological examination and assessment of cardiac function of LV

At the end of this investigation, two of the seven rats in the MI group exhibited a moderate thoracic adhesion, whereas only minimal thoracic adhesions were observed in the CHS group. The infarct zones and scar tissues in the LVs in the study groups were assessed using Masson's trichrome (MT) staining to label collagen scar tissues and cardiac muscle (which are represented by a dotted red line and a solid red line, respectively, in Fig. 4(a) and (b)). According to the MT stains, the chitosan-HYA/SF patches adhered strongly to the epicardial surfaces of the MI hearts, and they could markedly reduce the fibrosis in the infarcted zones below those in the MI group (Fig. 4(a) and (b), respectively). The result of MI staining of LV by implanting the patches in this investigation were similar to those in other reports although their results were obtained by implanting synthetic polymer patches or scaffolds into the MI hearts (Fujimoto et al., 2007; Jin et al., 2009; Miyahara et al., 2006; Piao et al., 2007). Additionally, to assess LV function, a series of echocardiographs were obtained to determine LVFS values. MI hearts that were implanted with chitosan-HYA/SF patches had a significantly higher LVFS ($P < 0.05$, $n = 8$, respectively) than the hearts in the MI group (Table 1). For example, the LVFS values in the CHS and MI groups were $42.8 \pm 2.4\%$ and $31.5 \pm 1.4\%$, respectively, ($n = 8$, for each group). Moreover, the end diastolic LV dimensions

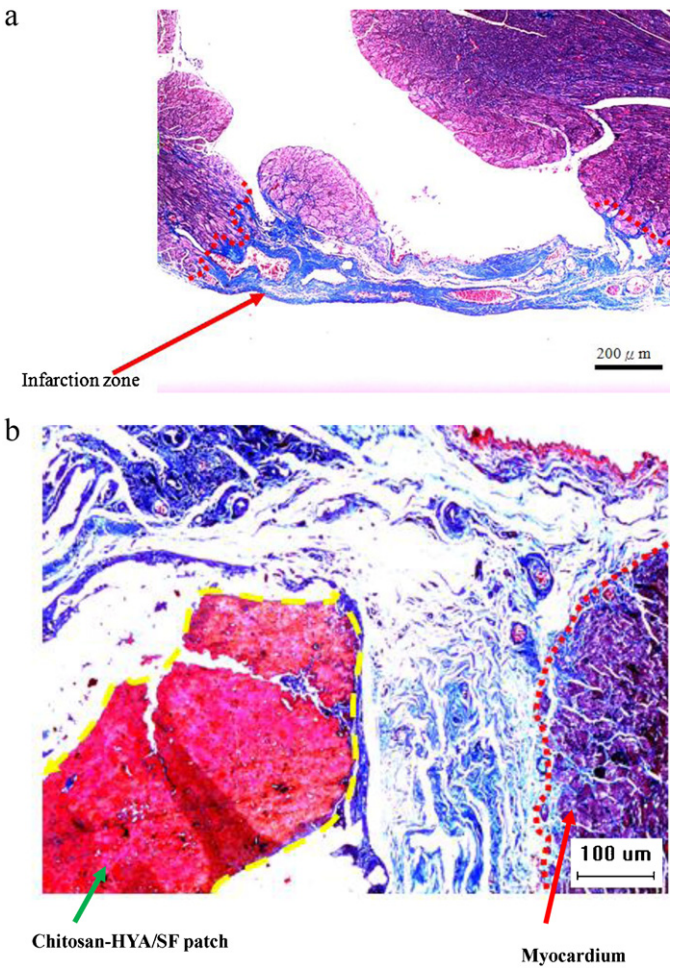

Fig. 4. Histological analyses by MT stains for (a) MI and (b) CHS groups in the MI regions of hearts for eight weeks of post-MI. Yellow spot line in 4(b) indicates the boundary of CS-HA/SF patches and MI regions, respectively. (For interpretation of the references to color in this figure legend, the reader is referred to the web version of this article.)

of the CHS group (5.2 ± 0.2 mm, $n = 8$) were significantly smaller than those of the MI group (6.2 ± 0.1 mm, $n = 8$). The end systolic LV dimensions of the CHS group (2.4 ± 0.2 mm, $n = 8$) were also significantly smaller than those of the MI group (3.7 ± 0.1 mm, $n = 8$). Accordingly, implanting chitosan-HYA/SF patches into MI hearts attenuated LV remodeling of post-MI in a 2-month study. Moreover, the LV walls in the CHS group (1.5 ± 0.13 mm, $n = 8$) were significantly thicker ($P < 0.05$, $n = 8$) than those in the MI group (Table 1). The improvements in the remodeling of the LVs in MI hearts that were made by implanting chitosan-HYA/SF patches were similar to those achieved in other investigations that utilized various synthetic scaffolds or hydrogels (Jin et al., 2009; Leor et al., 2009; Lin et al., 2010; Lu et al., 2010; Piao et al., 2007).

3.3. VWF Immuno-histological staining in MI regions

Fig. 5(a)–(c) shows the VWF staining of MI zones of the LVs in the study groups. Fig. 5(a) reveals numerous vWF-positive or vasculature structures in MI zone of LV in the sham group but only few ones were found in the MI group (Fig. 5(b)). Interestingly, some vWF-positive cells and neo-vascular structures (or blood vessel-like structures) were widely distributed in the MI zone of LV of the CHS group (Fig. 5(c)). Hence, implantation of the chitosan-HYA/SF patches for treating MI hearts strongly promoted the angiogenesis of the MI zones of LVs, whereas the implantation of PLCL scaffolds

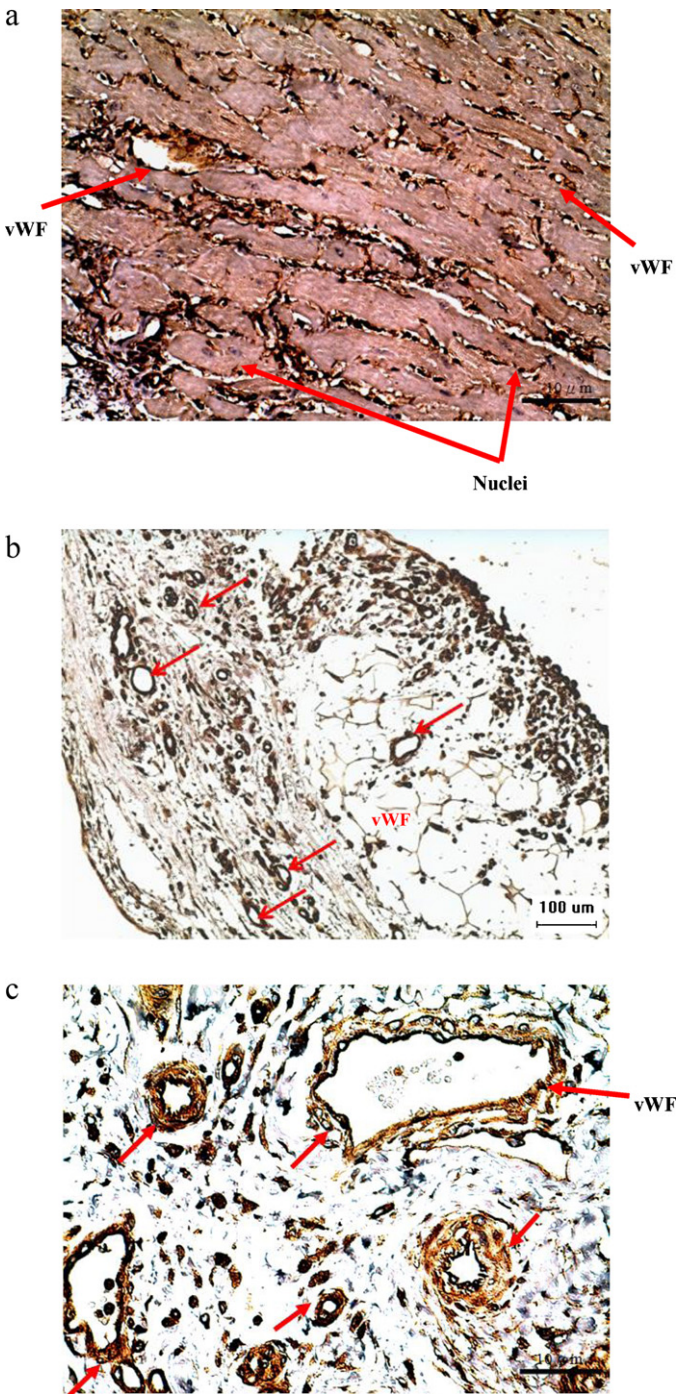

Fig. 5. IHC staining of vWF in the regions of LVs of the (a) Sham, (b) MI, and (c) CHS groups (×400). In the staining, the brown and black stains indicate vWF positive and nuclei of the cells, respectively. Numerous vWF positive cells and vessels were homogeneous distributed in the regions of LVs in the sham group while few vWF positive cells were found in the MI regions of LVs in the MI group. Blood vessel-like structures with vWF positive cells were widely distributed in the MI regions of LVs in the CHS group. (For interpretation of the references to color in this figure legend, the reader is referred to the web version of this article.)

generally did not (Fujimoto et al., 2007; Jin et al., 2009). These elastic PLCL scaffolds only provided mechanical support over the 2-month-long studying period (Fujimoto et al., 2007; Jin et al., 2009). The results of attenuating LV remodeling in the MI hearts such as the increase in LVFS values (Table 1) and the promotion of angiogenesis (Fig. 5(c)) achieved by implanting chitosan-HYA/SF patches demonstrate that the patches were both as mechanical supports and bio-chemically effective on cardiac repairs. The promotion of angiogenesis in MI hearts by treating them with chitosan-HYA/SF patches may result from the presence of chitosan-HYA components in the patches, which may influence the resident cardiac stem cells or recruit influent stem cells to MI regions, inducing angiogenesis and promoting myocardial reconstruction in infarcted hearts (Lu et al., 2010; Muzzarelli, 2011; Perng et al., 2011).

Table 2
Real-time PCR analyses for the gene expressions of (a) VEGF, (b) bFGF and (c) HGF factors in the MI regions of LVs of the study groups were shown. The values of the CHS group were significantly higher than those of the MI groups. ($^{*}P < 0.05$; $^{**}P < 0.01$; $n = 4$ for each group, respectively).

	VEGF	bFGF	HGF
MI group ($n = 4$) (assigned value)	1.0	1.0	1.0
CHS group ($n = 4$)	$2.19 \pm 0.11^{**}$	$2.23 \pm 0.29^{**}$	$4.85 \pm 0.21^{***}$

3.4. Expressions of paracrine factors in MI zones with implanting patches

VEGF is a cyto-protective and mitogenic factor for cardiomyocytes and also contributes to postnatal neo-vascularization by endothelial progenitor cells (Herrmann et al., 2011). Additionally, VEGF promotes myocardial protection in the short term by weakening the apoptotic signaling of cardiomyocytes and in the long-term by promoting neo-vascularization and tissue perfusion (Wang et al., 2010). bFGF promotes the proliferation of endothelial cells and their physical organization into tube-like structures. bFGF therapy reportedly improves the arteriogenic and echocardiographic parameters of LV functions in chronic pig ischemia (Kardestuncer et al., 2006; Meinel et al., 2005). HGF binds to tyrosine kinase receptors on vascular endothelial cells and affects their migration, proliferation, invasion, and neo-vascularization (Chi et al., 2012; Kardestuncer et al., 2006). In this work, the expressions of the gene markers of those paracrine factors in the MI regions were examined by RT-PCR. The expressions of VEGF, bFGF and HGF in the MI zones in the CHS group were significantly higher ($P < 0.05$ or better, $n = 4$) than those in the MI group (Table 2). For example, the values of VEGF in the MI and CHS groups were 1.0 and 2.19 ± 0.11 ($n = 4$, for each group), respectively. Accordingly, bFGF and HGF gene expressions in the treated MI zones in the CHS group were 2.23 ± 0.29 and 4.85 ± 0.21 ($n = 4$, for each group), respectively, but 1.0 (an assigned value) in the MI group. Hence, treating MI rat hearts with chitosan-HYA/SF patches significantly stimulated the expressions of VEGF, bFGF and HGF, resulting in more effective angiogenesis than in the MI group. The expressions of the paracrine factors in the treatments of MI hearts using chitosan-HYA/SF patches were greater than those achieved using synthetic scaffolds or patches (Fujimoto et al., 2007; Jin et al., 2009; Piao et al., 2007).

4. Conclusions

The cardiac repair of myocardial infarction (MI) hearts of rats using new chitosan-HYA/SF cardiac patches was examined after eight weeks of study. The patches significantly improved LV functions in MI hearts with markedly reducing the dilation of LVs, increasing the thickness of their walls and improving their fractional shortening (LVFS) in the CHS group, relative to those in the MI group. Moreover, the patches significantly improved angiogenesis in MI regions of LVs in the CHS group since staining revealed that the capillary-like structures were widely distributed in the regions but they were sparse in the MI group. The PCR analysis showed that the MI regions of LVs in the CHS group secreted more VEGF, bFGF and HGF in the regions than those in the MI group. Accordingly, new chitosan-HYA/SF cardiac patches promoted the cardiac

repairs of MI rat hearts although investigations of large quantities of rats need to be conducted in future.

Acknowledgements

The authors would like to thank the National Science Council of the Republic of China, Taiwan, for financially supporting this research under Contract Nos. NSC-100-2221-E-224-007 and 100-2314-B-002-047. Ted Knoy is appreciated for his editorial assistance.

References

Callegari, A., Bollini, S., Iop, L., Chiavegato, A., Torregrossa, G., Pozzobon, M., et al. (2007). Neo-vascularization induced by porous collagen scaffold implanted on intact and cryoinjured rat hearts. *Biomaterials*, *28*(36), 5449–5461.

Chi, N. H., Yang, M. C., Chung, T. W., Chen, J. Y., Chou, N. K., & Wang, S. S. (2012). Cardiac repair achieved by bone marrow mesenchymal stem cells/silk fibroin/hyaluronic acid patches in a rat of myocardial infarction model. *Biomaterials*, *33*, 5541–5551.

Dechert, T. A., Ducale, A. E., Ward, S. I., & Yager, D. R. (2006). Hyaluronan in human acute and chronic dermal wounds. *Wound Repair and Regeneration*, *14*(3), 252–258.

Fujimoto, K. L., Tobita, K., Merryman, W. D., Guan, J., Momoi, N., Stolz, D. B., et al. (2007). An elastic, biodegradable cardiac patch induces contractile smooth muscle and improves cardiac remodeling and function in subacute myocardial infarction. *Journal of the American College of Cardiology*, *49*(23), 2292–2300.

Herrmann, J. L., Abarbanell, A. M., Weil, B. R., Manukyan, M. C., Poynter, J. A., Brewster, B. J., et al. (2011). Optimizing stem cell function for the treatment of ischemic heart disease. *Journal of Surgical Research*, *166*(1), 138–145.

Jin, J., Jeong, S. I., Shin, Y. M., Lim, K. S., Shin, H., Lee, Y. M., et al. (2009). Transplantation of mesenchymal stem cells within a poly(lactide-co-epsilon-caprolactone) scaffold improves cardiac function in a rat myocardial infarction model. *European Journal of Heart Failure*, *11*(2), 147–153.

Kardestuncer, T., McCarthy, M. B., Karageorgiou, V., Kaplan, D., & Gronowicz, G. (2006). RGD-tethered silk substrate stimulates the differentiation of human tendon cells. *Clinical Orthopedics and Related Research*, *448*, 234–239.

Kochupura, P. V., Azeloglu, E. U., Kelly, D. J., Doronin, S. V., Badylak, S. F., Krukenkamp, I. B., et al. (2005). Tissue-engineered myocardial patch derived from extracellular matrix provides regional mechanical function. *Circulation*, *112*(9 Suppl.), I144–I149.

Leor, J., Tuvia, S., Guetta, V., Manczur, F., Castel, D., Willenz, U., et al. (2009). Intracoronary injection of in situ forming alginate hydrogel reverses left ventricular remodeling after myocardial infarction in Swine. *Journal of the American College of Cardiology*, *54*(11), 1014–1023.

Li, R. K., Jia, Z. Q., Weisel, R. D., Mickle, D. A., Zhang, J., Mohabeer, M. K., et al. (1996). Cardiomyocyte transplantation improves heart function. *The Annals of Thoracic Surgery*, *62*(3), 654–660.

Lin, Y. D., Yeh, M. L., Yang, Y. J., Tsai, D. C., Chu, T. Y., Shih, Y. Y., et al. (2010). Intramyocardial peptide nanofiber injection improves postinfarction ventricular remodeling and efficacy of bone marrow cell therapy in pigs. *Circulation*, *122*(11 Suppl.), S132–S141.

Lu, S., Wang, H., Lu, W., Liu, S., Lin, Q., Li, D., et al. (2010). Both the transplantation of somatic cell nuclear transfer- and fertilization-derived mouse embryonic stem cells with temperature-responsive chitosan hydrogel improve myocardial performance in infarcted rat hearts. *Tissue Engineering Part A*, *16*(4), 1303–1315.

Meinel, L., Hofmann, S., Karageorgiou, V., Kirker-Head, C., McCool, J., Gronowicz, G., et al. (2005). The inflammatory responses to silk films in vitro and in vivo. *Biomaterials*, *26*(2), 147–155.

Minatoya, K., Kobayashi, J., Sasako, Y., Ishibashi-Ueda, H., Yutani, C., & Kitamura, S. (2001). Long-term pathological changes of expanded polytetrafluoroethylene (ePTFE) suture in the human heart. *Journal of Heart Valve Disease*, *10*(1), 139–142.

Miyahara, Y., Nagaya, N., Kataoka, M., Yanagawa, B., Tanaka, K., Hao, H., et al. (2006). Monolayered mesenchymal stem cells repair scarred myocardium after myocardial infarction. *Nature Medicine*, *12*(4), 459–465.

Muzzarelli, R. A. A., Mattioli-Belmonte, M., Tietz, C., Biagini, R., Ferioli, G., Brunelli, M. A., et al. (1994). Stimulatory effect on bone formation exerted by a modified chitosan. *Biomaterials*, *15*, 1075–1081.

Muzzarelli, R. A. A. (2009). Chitins and chitosans for the repair of wounded skin, nerve, cartilage and bone. *Carbohydrate Polymers*, *76*, 167–182.

Muzzarelli, R. A. A. (2011). Chitosan composites with inorganics, morphogenetic proteins and stem cells, for bone regeneration. *Carbohydrate Polymers*, *83*(4), 1433–1445.

Muzzarelli, R. A. A. (2012). Chitosan, hyaluronan and chondroitin sulfate in tissue engineering for cartilage regeneration: A review. *Carbohydrate Polymers*, *89*, 723–739.

Nelson, D. M., Ma, Z., Fujimoto, K. L., Hashizume, R., & Wagner, W. R. (2011). Intramyocardial biomaterial injection therapy in the treatment of heart failure: Materials, outcomes and challenges. *Acta Biomaterialis*, *7*(1), 1–15.

Perng, C. K., Wang, Y. J., Tsi, C. H., & Ma, H. (2011). In vivo angiogenesis effect of porous collagen scaffold with hyaluronic acid oligosaccharides. *Journal of Surgical Research*, *168*(1), 9–15.

Piao, H., Kwon, J. S., Piao, S., Sohn, J. H., Lee, Y. S., Bae, J. W., et al. (2007). Effects of cardiac patches engineered with bone marrow-derived mononuclear cells and PGCL scaffolds in a rat myocardial infarction model. *Biomaterials*, *28*(4), 641–649.

Pinhasov, A., Mei, J., Amaratunga, D., Amato, F. A., Lu, H., Kauffman, J., et al. (2004). Gene expression analysis for high throughput screening applications. *Combinatorial Chemistry and High Throughput Screening*, *7*(2), 133–140.

Rios, C. N., Skoracki, R. J., Miller, M. J., Satterfield, W. C., & Mathur, A. B. (2009). In vivo bone formation in silk fibroin and chitosan blend scaffolds via ectopically grafted periosteum as a cell source: A pilot study. *Tissue Engineering Part A*, *15*(9), 2717–2725.

Robinson, K. A., Li, J., Mathison, M., Redkar, A., Cui, J., Chronos, N. A., et al. (2005). Extracellular matrix scaffold for cardiac repair. *Circulation*, *112*(9 Suppl.), I135–I143.

Treguer, F., Donal, E., Tamareille, S., Ghaboura, N., Derumeaux, G., Furber, A., et al. (2010). Speckle tracking imaging improves in vivo assessment of EPO-induced myocardial salvage early after ischemia-reperfusion in rats. *The American Journal of Physiology—Heart and Circulatory Physiology*, *298*(6), H1679–H1686.

Van den Bos, E. J., Mees, B. M., de Waard, M. C., de Crom, R., & Duncker, D. J. (2005). A novel model of cryoinjury-induced myocardial infarction in the mouse: A comparison with coronary artery ligation. *The American Journal of Physiology—Heart and Circulatory Physiology*, *289*(3), H1291–H1300.

Van Lenthe, F. J., Gevers, E., Joung, I. M., Bosma, H., & Mackenbach, J. P. (2002). Material and behavioral factors in the explanation of educational differences in incidence of acute myocardial infarction: The Globe study. *Annals of Epidemiology*, *12*(8), 535–542.

Wang, S., Zhang, Z., Lin, X., Xu, D. S., Feng, Y., & Ding, K. (2010). A polysaccharide, MDG-1, induces S1P1 and bFGF expression and augments survival and angiogenesis in the ischemic heart. *Glycobiology*, *20*(4), 473–484.

Yamazaki, Y., Eguchi, S., Miyamura, H., Hayashi, J., Fukuda, J., Ozeki, H., et al. (1989). Replacement of myocardium with a Dacron prosthesis for complications of acute myocardial infarction. *The Journal of Cardiovascular Surgery*, *30*(2), 277–280.

Yang, M. C., Wang, S. S., Chou, N. K., Chi, N. H., Huang, Y. Y., Chang, Y. L., et al. (2009). The cardiomyogenic differentiation of rat mesenchymal stem cells on silk fibroin-polysaccharide cardiac patches in vitro. *Biomaterials*, *30*(22), 3757–3765.

Yang, M. C., Chi, N. H., Chou, N. K., Huang, Y. Y., Chung, T. W., Chang, Y. L., et al. (2010). The influence of rat mesenchymal stem cell CD44 surface markers on cell growth, fibronectin expression, and cardiomyogenic differentiation on silk fibroin—Hyaluronic acid cardiac patches. *Biomaterials*, *31*(5), 854–862.

Yang, Z. J., Ma, D. C., Wang, W., Xu, S. L., Zhang, Y. Q., Chen, B., et al. (2007). Neovascularization and cardiomyocytes regeneration in acute myocardial infarction after bone marrow stromal cell transplantation: Comparison of infarct-relative and noninfarct-relative arterial approaches in swine. *Clinica Chimica Acta*, *381*(2), 114–118.